Lymphatic magnetic resonance imaging abnormalities in children with repaired tetralogy of Fallot

Thomas Holm-Weber[1] [ORCID], Sheyanth Mohanakumar[2], Thora Wesenberg Helt[3], Lotte Borgwardt[4], Lise Borgwardt[3], Klaus Juul[5], Vibeke B. Christensen[5,6] and Vibeke E. Hjortdal[1]

[1]Department of Thoracic Surgery, Rigshospitalet, Copenhagen, Denmark; [2]Department of Radiology, Aarhus University Hospital, Aarhus, Denmark; [3]Department of Clinical Physiology & Nuclear Medicine, Rigshospitalet, Copenhagen, Denmark; [4]Department of Diagnostic Radiology, Rigshospitalet, Copenhagen, Denmark; [5]Department of Pediatrics and Adolescent Medicine, Rigshospitalet, Copenhagen, Denmark and [6]Comparative Pediatrics and Nutrition, Copenhagen University, Copenhagen, Denmark

Abstract

Introduction: Tetralogy of Fallot patients face an elevated risk of developing chylothorax and pleural effusions post-surgery. This patient group exhibits risk factors known to compromise the lymphatic system, such as elevated central venous pressure, pulmonary flow changes, and hypoxia. This study investigates the morphology and function of the lymphatic system in tetralogy of Fallot patients through lymphatic magnetic resonance imaging and near-infrared fluorescence imaging, respectively. *Methods:* Post-repair tetralogy of Fallot patients aged 6–18 years were recruited, along with age and gender-matched controls. Magnetic resonance imaging was used to assess the morphology of the thoracic lymphatic vessels and the thoracic, while near-infrared fluorescence imaging was used to assess lymphatic activity utilising lymph rate, velocity, and pressure. *Results:* Nine patients and 10 controls were included. Echocardiography revealed that 2/3 of the patients had moderate-severe pulmonary regurgitation, while none displayed signs of elevated central venous pressure. Magnetic resonance imaging identified three patients with type 3 (out of 4 types) lymphatic abnormalities, while controls had none. The thoracic ducts showed severe (one patient) and moderate (one patient) tortuosity. Mean thoracic duct diameters were 3.3 mm ±1.1 in patients and 3.0 mm ± 0.8 in controls (p-value = 0.53). Near-infrared fluorescence imaging revealed no anomalous patterns. *Conclusion:* Despite no presence of clinical lymphatic disease, 3/9 of the repaired tetralogy of Fallot patients exhibited lymphatic morphological abnormalities. The significance of these anomalies remains uncertain currently. Further research is needed to determine whether these lymphatic alterations in this patient cohort are a result of congenital malformations, haemodynamic shifts, or prenatal and early-life saturation levels.

Introduction

Tetralogy of Fallot patients face higher risk than most congenital heart disease patients of developing chylothorax (4%) and pleural effusions (7%) after surgical repair.[1,2] Both conditions are severe comorbidities as they prolong intensive care unit stays.[3] The accumulated fluid during chylothorax contains fatty substances absorbed from the small intestines originating from the lacteals. This contrasts the accumulated fluid during serous pleural effusions, which contain serous fluid. Chylothorax fluid is characterised by a milky-white appearance, in contrast to the clear appearance of non-chylous pleural effusions. Chylothorax may be a result of traumatic injury during surgery,[4] whereas pleural effusions develop when the lymphatic system fails to reabsorb sufficient fluid. This can be instigated by various peri-surgical factors, such as alterations in haemodynamics, inflammation, preoperative oxygen levels, and the duration of mechanical ventilator use.[5,6] Additionally, patients with tetralogy of Fallot live with elevated right atrial pressures, which are associated with the severity of the disease, higher mortality rates,[7] and compromises the lymphatic system's ability to return lymphatic fluid to the central venous system.[8] While the haemodynamics in patients with tetralogy of Fallot is well described,[9] the lymphodynamics remain to be explored. Children diagnosed with tetralogy of Fallot manifest characteristics that can potentially impact the lymphatic system from the prenatal period till after the surgical repair. These manifestations include prenatal cyanosis,[10] alterations in pulmonary blood flow,[11] and elevated central venous pressures following the surgical repair.[7,12] It is currently unclear whether paediatric patients with tetralogy of Fallot with no clinical lymphatic diseases exhibit abnormalities within their lymphatic system. This study

CAMBRIDGE
UNIVERSITY PRESS

aimed to examine if paediatric patients after surgical repair of tetralogy of Fallot have signs of subclinical abnormalities of the lymphatic system. To accomplish this, we evaluated lymphatic morphology and dynamics using two distinct methods: lymphatic MRI and near-infrared fluorescence imaging. Lymphatic MRI evaluates the morphology of lymphatic vessels, using a T2-weighted setting to capture the lymphatic vessels by detecting the signal from the slow or still standing fluid from within the lymphatic vessels. Whereas near-infrared fluorescence imaging offers real-time visualisation of lymphatic vessels, providing a dynamic and immediate assessment.

Materials and methods

Recruitment

Controls and patients who had undergone tetralogy of Fallot repair between 6 and 18 years of age were eligible to participate in this study, and 39 patient families were contacted (Figure 1 Supplementary). The healthy controls were recruited through the network of collaborators of the study. The patient records were reviewed to assess the surgical and medical history of the tetralogy of Fallot patients. To evaluate potential subclinical indicators of lymphatic disease, blood tests were drawn.

Lymphatic MRI

The lymphatic anatomy of the neck (C2) to the diaphragm was acquired using a 1.5-T MRI system (GE Optima™ MR450w, GE Healthcare). The patient was placed supine, and multi-array radiofrequency coils were used. The lymphatic system was imaged using a procedure that involved coronal slices acquired with a respiratory-gated (navigator) 3-dimensional fast T2-weighted fast spin-echo sequence. This setting captures slow or still-standing fluid, enabling the investigator to detect the fluid within the lymphatic vessels. The typical imaging parameters were field of view 450×450 mm; pixel size, $1.1 \times 1.1 \times 1.0$ mm; echo time, 700 ms; slice thickness, 2 mm.

Lymphatic near-infrared fluorescence imaging

The lymphatic activity was recorded using the Kaers Imaging System (Kaer Labs, Nantes, France.) Initially, indocyanine green was injected into the first and fourth interdigital spaces. The injected dye underwent excitation through a laser, triggering the emission of light upon the dye's subsequent stabilisation. This emitted light was then captured by a custom-made camera, enabling the investigator to identify the lymphatic vessels. After 15 min of lying down, the lymph rate and velocity were measured (sequence 1), followed by the measurement of lymph pressure (sequence 2), and finally, the lymph rate and velocity 2 were obtained (sequence 3) (Figure 2 Supplementary).

Lymph pressure was determined by occluding lymphatic flow using a Hokanson sphygmomanometer cuff (ADInstruments, Oxford, UK) after manually emptying the lymph vessels. The procedure involved placing a tourniquet on the calf, manually removing the dye by compressing the lymphatic vessels, inflating the cuff to 80 mmHg, and gradually reducing cuff pressure by 10 mmHg every fifth minute until the highest pressure at which the fluorescent dye passed the inflatable cuff was recorded as the lymph pressure.

Echocardiography

Standard echocardiographic measurements were performed by a single echocardiographer (KJ). The central venous pressure was estimated and grouped as: normal (5 mmHg), mildly increased (5–10 mmHg), moderately increased (10–15 mmHg), and severely increased (>15 mmHg). These estimates were determined based on the dilation of the inferior vena cava compared to the abdominal aorta, which could be non-dilated with inspiratory collapse, non-dilated with reduced inspiratory collapse, dilated with some inspiratory collapse, or dilated with no inspiratory collapse, respectively. Z-scores for tricuspid annular plane systolic excursion were calculated using the Boston Children's Hospital reference material (https://zscore.chboston.org/).

Data analysis

Lymphatic MRI

The MRI sequences were analysed using Horos™ (Horos Project, Geneva, Switzerland). Three parameters were used to assess the lymphatic vessels.

Lymphatic abnormality score. The classification system proposed by Biko et al. was employed to evaluate the lymphatic abnormality in pre-Fontan patients. The scores range from 1 to 4.[13] Type 1 is interpreted as showing minimal or no presumed lymphatic channels within both the supraclavicular region and mediastinum (Figure 3.1 Supplementary). Type 2 exhibits abnormal elevation in lymphatic channels, specifically within the supraclavicular region, without any extension into the mediastinum (Fig 3.2 Supplementary). Type 3 displays abnormal supraclavicular lymphatics, with evident extension into the mediastinum (Fig 3.3 Supplementary). Type 4 displays abnormal supraclavicular lymphatic vessels extending into both the mediastinum and the lung parenchyma. Type 4 was associated with poorer outcomes after Fontan completion. The analysis was carried out by two investigators (TH and SM). In instances where there were discordant scores between the investigators, the sequences were reevaluated, and a final score was reached through mutual consensus.

Thoracic duct. The thoracic duct was assessed by tortuosity and diameter following the same approach as Castellanos et al.[14] Thoracic duct tortuosity was determined using the following criteria: none, no turns or deviations; mild, one turn or subtle turns; moderate, multiple large turns or several small turns; and severe, turns along almost the entire course. The maximum diameter of the thoracic duct was ascertained by locating its largest segment in the coronal plane and then measuring it using a short-axis view.

Lymphatic near-infrared imaging

Lymphatic near-infrared imaging was solely utilised in the tetralogy of Fallot group to extract lymph rate, velocity, and pressure.[15–17] Lymph rate and velocity were extracted using a custom LabView program (National Instruments, TX, U.S.). Lymph rate was determined as the number of lymphatic contractions generated per vessel per min, with analysis of all visible vessels and pooling of the mean contraction rate for each sequence. Lymph velocity was determined by measuring the velocity of lymph propulsion in cm/s.

ImageJ[18] was used to determine lymph pressure; the lymph pressure was defined as the maximum pressure the lymphatic

Table 1. Surgical history and MRI findings of the tetralogy of Fallot patients

ID	Age	Sex	Pre repair			Repair		Post repair		MR findings		
			Anatomy	SAT (\%)	Shunted	Age_1	Repair	Revalved	PR	Type	Tortuosity	ø
A	9	F	ToF PA	NA	–	0.8	TAP	No	6.0	1	None	2.8
B	17	M	ToF PA	70–75	3	3.0	Contegra graft	Yes	4.0	3	Moderate	4.8
C	10	F	ToF	96–100	–	9.0	TAP	No	10.0	2	None	2.5
D	6	M	ToF	96–100	–	6.0	TAP	No	6.0	1	Mild	2.0
E	17	M	ToF PA	76–80	8	7.0	TAP	Yes	15.5	1	Mild	3.4
F	13	F	ToF	86–90	–	14.0	TAP	Yes	13.0	1	Not visualised	–
G	6	F	ToF	91–95	–	8.0	TAP	No	2.0	3	Severe	3.6
H	16	F	ToF PA w/ MAPCA	70–75	–	7.0	Contega graft	No	15.5	2	Mild	5.2
I	11	M	ToF PA	81–85	18	19.0	TAP	No	9.5	3	Mild	2.5

Age in years. Sex: F = female, M = male. Pre repair: ToF= tetralogy of Fallot; PA = pulmonary atresia; MAPCA = major aortopulmonary collateral arteries; Sat = saturations before repair; Shunted = number of months with palliative mBTT shunt. Repair: Age = months old at surgical repair; Repair = type of surgical repair; TAP = transannular patch. Post repair: Revalved = revalved after primary repair; PR = years with pulmonary regurgitation. MRI findings: Type: lymphatic MRI scoring according to Biko et al.[13] Tortuosity = tortuosity of the thoracic duct; ø = diameter of the thoracic duct (mm). One patient (C) had DiGeorge syndrome; the rest of the patients had no record of genetic disorders. Two patients (C + E) experienced prolonged pleural effusions. No additional history or current evidence of lymphatic disorders was revealed. NA = not available.

vessels could overcome in mmHg following the same procedure as prior studies.[15,16,19]

Statistical analyses

Continuous variables are presented with means and standard deviations, while categorical variables are presented as frequencies. Student *t*-test was used to compare the tetralogy of Fallot participants to controls and non-participants. All statistical analyses were performed using R Core Team (2022). (R: A language and environment for statistical computing. R Foundation for Statistical Computing, Vienna, Austria. URL https://www.R-project.org/).

Results

Study population

Nine out of the 39 invited patients accepted to participate in the study after parental consent was obtained. The baseline characteristics of both the control (age 11 ± 3 years, 50% female) and patient (age 12 ± 4 years, 44% female) groups are presented in (Supplementary Table 1). All examinations of each participant were conducted within 2 days, except for patient H, where the echocardiography was performed 1 month after the lymphatic MRI. All 9 patients have had pulmonary regurgitation at some time during their lives and the years exposed to pulmonary regurgitation varied from 2 to 15.5 years (Table 1) The examinations were conducted, on average, 11.6 ± 4 years following tetralogy of Fallot repair. Seven out of nine patients underwent transannular patch repair. Except for one patient diagnosed with DiGeorge syndrome (patient C), no other relevant comorbidities were identified within the patient group. Echocardiography revealed 5 of the 9 patients with tetralogy of Fallot exhibited severe pulmonary regurgitation at the time of investigation, while none displayed signs of elevated central venous pressure. (Supplementary Table 2) The invited tetralogy of Fallot patients who chose not to participate in the study had similar characteristics regarding age, sex, body size, or surgical history. (Supplementary Table 3) Data from the medical records showed that following tetralogy of Fallot repair,

one patient had an extended stay in the intensive care unit due to right ventricle failure, while two patients experienced prolonged pleural effusion. Two patients had a valved conduit as the primary repair. Three patients were later revalved, one patient shortly after primary repair, and two patients during adolescence. No patients experienced chylothorax, oedema, protein-losing enteropathy, or ascites. Blood tests drawn during this study revealed no severely abnormal findings in either group (Supplementary Table 4,5).

Lymphatic MRI and near-infrared fluorescence imaging

MRI revealed three patients with type 3 lymphatic abnormalities in the patient group versus none in the control group (Figure 1, 2). The thoracic ducts were moderately tortuous in another patient (patient B) and severely tortuous in one patient (patient G). No controls displayed severe or moderate thoracic duct tortuosity (Table 1). The mean thoracic duct diameters were 3.3 mm ± 1.1 and 3.0 mm ± 0.8 (*p*-value = 0.53) in the tetralogy of Fallot and control groups, respectively. The near-infrared fluorescence imaging investigations did not reveal any anomalous patterns (Supplementary Table 6).

Type 3 abnormal lymphatic vessels

The average duration between repair and lymphatic MRI was 11 years for patients exhibiting type 3 abnormal lymphatic vessels. Prior to repair, two out of three patients had low pre-repair saturations (Table 1). Moreover, within this specific subgroup, two patients (B and I) encountered complex trajectories both preceding and following the reparative interventions. Patients B and I underwent the application of the Blalock–Thomas–Taussig shunt palliation before repair. The Blalock–Thomas–Taussig shunt in patient B was subsequently replaced with another shunt before undergoing contegra graft repair, accompanied by subsequent dilations of the pulmonary arteries. On the other hand, patient G did not experience any significant surgical complications and received transannular patch repair. Patient I underwent placement of two Blalock–Thomas–Taussig shunts concurrently prior to the transannular patch repair. Patients G and I had severe pulmonary regurgitation at the time of the study. None of the patients had any
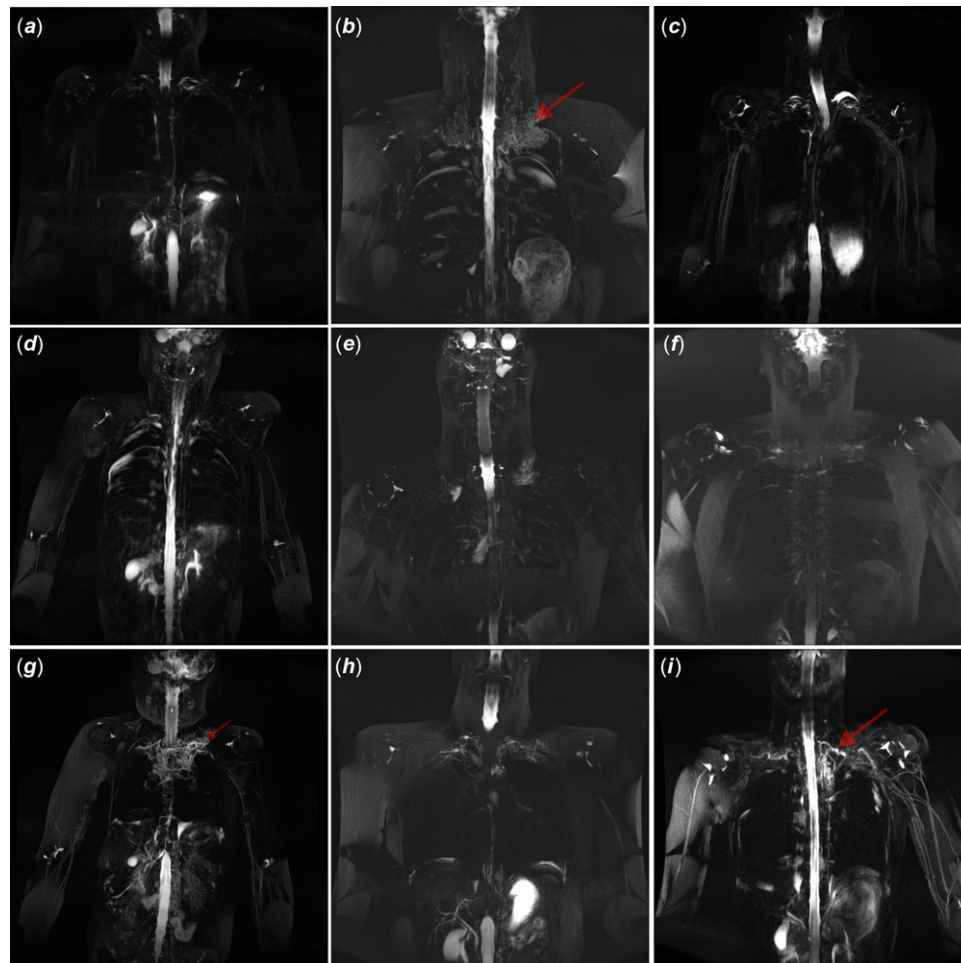
Figure 1. Tetralogy of Fallot.

symptoms of on-going lymphatic disease at the time of investigation or previously.

Discussion

We found abnormal lymphatic vessels (lymphatic MRI type 3) in three out of nine paediatric patients with tetralogy of Fallot, indicating some degree of lymphatic congestion. This is the first study to investigate the lymphatic state of children with tetralogy of Fallot using MRI and near-infrared fluorescence imaging.

Lymphatic congestion and pleural effusion in tetralogy of Fallot

The elevated central venous pressure observed in patients with tetralogy of Fallot[7] is a common risk factor for both lymphatic congestion[20] and pleural effusions.[3] The fluid accumulation seen in pleural effusions is the result of an imbalance between fluid filtration and removal by the lymphatic system. Patients with tetralogy of Fallot undergoing repair surgery may exhibit three risk factors (elevated central venous pressure, increases in pulmonary blood flow, and reduced pre-repair oxygen saturation levels) that may be associated with the development of lymphatic congestion and/or pleural effusion.

Haemodynamics

Increased central venous pressure. The increased risk of pleural effusions following tetralogy of Fallot repair[1] might be caused by restrictive right ventricle physiology. Restrictive right ventricle physiology increases the venous systemic pressure.[21] Increases in central venous pressure are known to impede the lymphatic system's ability to return lymphatic fluid to the venous system.[8] In patients with Fontan circulation, central venous pressure is believed to be a main component of the pathophysiology, leading to an increase in afterload on the lymphatic system and lymphatic congestion.[22] This is thought to be the cause of a depressed lymphatic capacity in patients with Fontan circulation.[19] These patients are at risk of developing lymphatic disorders like protein-losing enteropathy, chylothorax, ascites, and plastic bronchitis.[22] However, severe lymphatic issues are rare in tetralogy of Fallot patients and have only been observed in case studies.[23,24] None of our patients showed echocardiographic signs of elevated central venous pressure. However, during various stages of their surgical history leading up to valve replacement, there might have been periods when their central venous pressure was elevated. Each of our patients encountered some level of pulmonary regurgitation at some point in their lives, and at the time of this study, 2/3 of the patients continued to experience pulmonary regurgitation. Additionally, among patients with type 3 abnormal lymphatic vessels observed on MRI, two out of three had severe pulmonary regurgitation. (Supplementary Table 2).
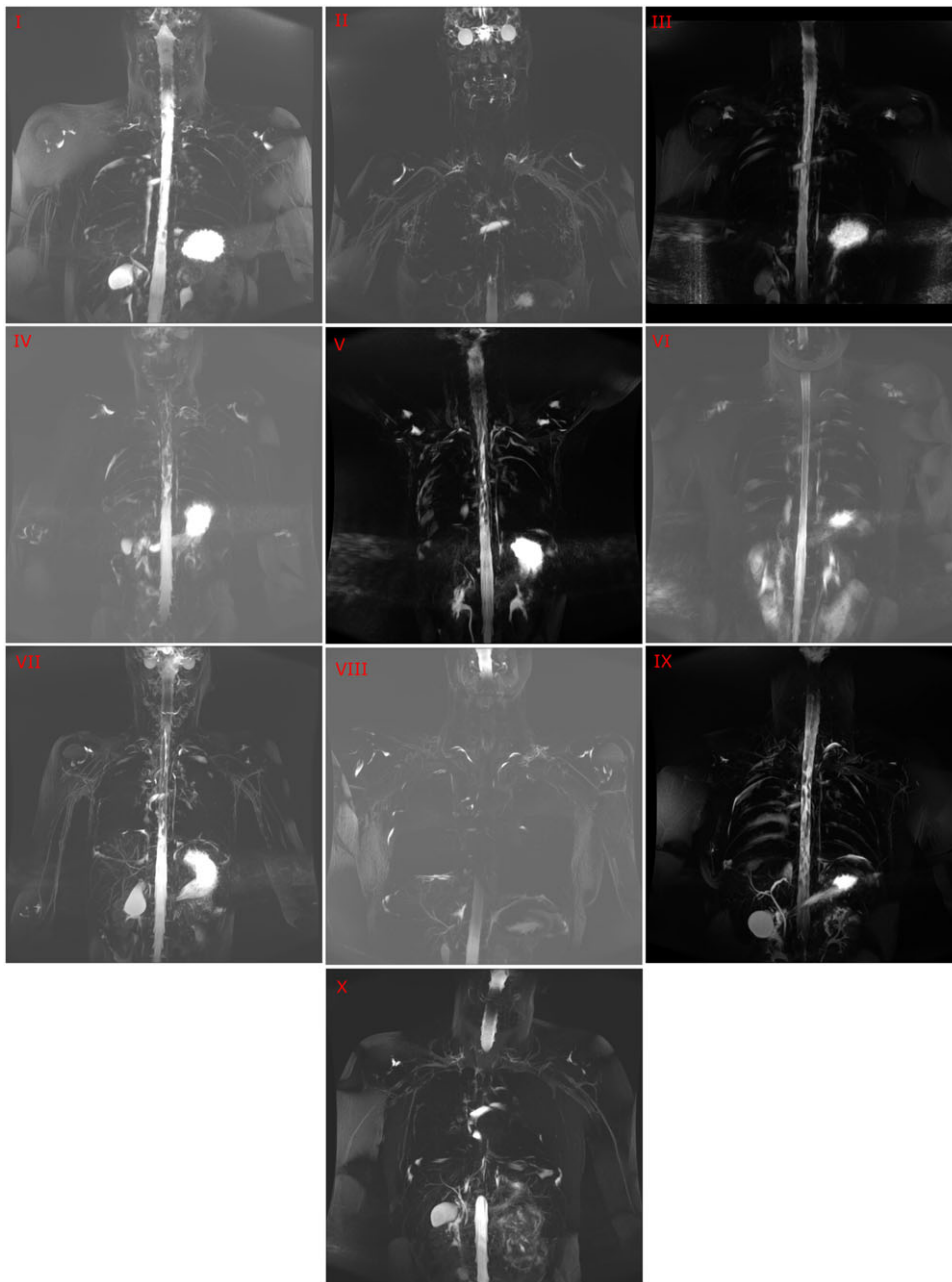
Figure 2. Tetralogy of Fallot.

Increased pulmonary flow. Ovine studies found that increases in pulmonary blood flow lead to impaired lymphatic drainage, dilation of lymphatic vessels, and increases in fluid filtration.[25,26] The increases in pulmonary blood flow in shunt palliated tetralogy of Fallot patients pre-repair and all tetralogy of Fallot patients after repair (compared to before repair) could contribute to the lymphatic congestion. In the tetralogy of Fallot group with type 3 lymphatic abnormalities, two out of three were shunt palliated up until repair (Table 2).

Hypoxia

During hypoxia, the extravasation increases, leading to an increase in lymph production and reabsorption.[27,28] Furthermore, basic research and animal models suggest that lymphangiogenesis is stimulated during hypoxia.[29,30] Most patients with tetralogy of Fallot are exposed to varying degrees of hypoxia before surgical repair. Even before birth, patients with tetralogy of Fallot are exposed to lower saturation levels.[10] These factors could also contribute to the development of abnormal lymphatic vessels compared with healthy controls. Two out of three in the tetralogy of Fallot group with type 3 lymphatic abnormalities had low systemic pre-repair saturations (Table 2).

Type 3 abnormal vessels

The group of patients with tetralogy of Fallot with type 3 abnormal vessels exhibited complex peri-surgical histories, severe pulmonary regurgitations, lower pre-repair saturations, and had been palliated with Blalock–Thomas–Taussig shunts (Table 2, Supplementary Table 2). All of which could potentially put a strain on the lymphatic system. The mean time from repair to lymphatic MRI was no different from the rest of the group, suggesting no

Table 2. Characteristics of the three tetralogy of Fallot patients exhibiting lymphatic MRI type 3 abnormal lymphatics concerning pre-repair, repair, and post-repair periods

	Pre repair			Repair		Post repair		
ID	Anatomy	SAT (\%)	Shunted (months)	Age (months)	Type	PR (years)	Tortousity	ø (mm)
B	ToF PA	70–75	3	3	Contegra graft	4.0	Moderate	5.0
G	ToF	91–95	–	8	TAP	2.0	Severe	2.3
I	ToF PA	81–85	18	19	TAP	9.5	Mild	2.7

ToF = tetralogy of Fallot, PA = pulmonary atresia, Sat = saturations before repair, Shunted = months of systemic–pulmonary shunting, Age = age in months at repair; TAP = transannular patch; PR = pulmonary regurgitation in years; ø = thoracic duct diameter (mm).

time-associated factors within the study. The absence of previous or present clinical signs of lymphatic congestion underlines the subclinical nature of the findings and is aligned with Biko et al's findings that Fontan patients only reported poorer outcome within the group with type 4 abnormalities.

Clinical impact

Currently, the clinical significance of the reported MRI findings indicating lymphatic congestion remains uncertain. In Fontan patients, lymphatic abnormalities are documented from infancy and seem to be associated with worse long-term outcomes.[31] In patients with tetralogy of Fallot, an anomalous lymphatic system could potentially be a part of the explanation as to why they face an increased risk of developing post-repair pleural effusion.

Limitations

The limited sample size and cross-sectional design prevent us from making definitive conclusions regarding the underlying patho-physiology of this observation. Additionally, it is important to note that near-infrared fluorescence imaging investigations exclusively visualise superficial lymphatic vessels, while deeper vessels may exhibit distinct characteristics. The lymphatic MRI has limitations, particularly in its inability to capture flow patterns, compared to the more invasive dynamic lymphatic MRI. Additionally, it is worth noting that our study lacked pre-repair MRI images for the patient group, further contributing to the range of limitations. Furthermore, the MRI evaluation of abnormal lymphatic vessels utilised scoring systems originally developed to assess lymphatic abnormalities in pre-Fontan patients, rather than in patients after Tetralogy of Fallot repair.

Conclusion

In this current study, 3 out of 9 repaired tetralogy of Fallot patients exhibited type 3 abnormal lymphatic vessels in the supraclavicular region and mediastinum. Furthermore, among these three patients, two displayed abnormal tortuosity of the thoracic duct, despite the absence of any clinical signs of lymphatic disease. The significance of these anomalies remains uncertain currently. Further research is needed to determine whether these lymphatic alterations in this patient cohort are a result of congenital malformations, haemodynamic shifts, or prenatal and early-life saturation levels.

References

1. Mavroudis CD, Mavroudis CD, Jacobs JP et al. Procedure-Based Complications to Guide Informed Consent: Analysis of Society of Thoracic Surgeons-Congenital Heart Surgery Database. Ann Thorac Surg 2014; 97: 1838–1851. DOI: 10.1016/j.athoracsur.2013.12.037.
2. Mouws EMJP, De Groot NMS, Van De Woestijne PC et al. Tetralogy of Fallot in the current era. Semin Thorac Cardiovasc Surg 2019; 31: 496–504. DOI: 10.1053/j.semtcvs.2018.10.015.
3. Vaynblat M, Chiavarelli M, Anderson JE, Rao S, Nudel DB, Cunningham JN. Pleural drainage after repair of Tetralogy of Fallot. J Card Surg 1997; 12: 71–76. DOI: 10.1111/J.1540-8191.1997.TB00097.X.
4. Doerr CH, Allen MS, Nichols FC, Ryu JH. Etiology of chylothorax in 203 patients. Mayo Clin Proc 2005; 80: 867–870. DOI: 10.4065/80.7.867.
5. Biondi JW, Schulman DS, Wiedemann HP, Matthay RA. Mechanical heart-lung interaction in the adult respiratory distress syndrome. Clin Chest Med 1990; 11: 691–714. DOI: 10.1016/s0272-5231(21)00763-2.
6. Talwar S, Agarwala S, Mittal CM, Choudhary SK, Airan B. Pleural effusions in children undergoing cardiac surgery. Ann Pediatr Cardiol 2010; 3: 58–64. DOI: 10.4103/0974-2069.64368.
7. Egbe AC, Connolly HM, Miranda WR, Scott CG, Borlaug BA. Prognostic implications of inferior vena cava haemodynamics in ambulatory patients with Tetralogy of Fallot. ESC Hear Fail 2020; 7: 2589–2596. DOI: 10.1002/ehf2.
8. Brace RA, Valenzuela GJ. Effects of outflow pressure and vascular volume loading on thoracic duct lymph flow in adult sheep. Am J Physiol - Regul Integr Comp Physiol 1990; 258: 27–21. DOI: 10.1152/ajpregu.1990.258.1.r240.
9. Bailliard F, Anderson RH. Tetralogy of Fallot. Orphanet J Rare Dis 2009; 4: 2. DOI: 10.1186/1750-1172-4-2.
10. Sun L, van Amerom JFP, Marini D et al. MRI characterization of hemodynamic patterns of human fetuses with cyanotic congenital heart

disease. Ultrasound Obstet Gynecol 2021; 58: 824–836. DOI: 10.1002/uog.23707.

11. Wise-Faberowski L, Asija R, McElhinney DB. Tetralogy of Fallot: Everything you wanted to know but were afraid to ask. Pediatr Anesth 2019; 29: 475–482. DOI: 10.1111/PAN.13569.

12. Egbe AC, Bonnichsen C, Reddy YNV, Anderson V, Borlaug JH, BA. Pathophysiologic and Prognostic Implications of Right Atrial Hypertension in Adults With Tetralogy of Fallot. J Am Heart Assoc 2019; 8: e014148. DOI: 10.1161/JAHA.119.

13. Biko DM, DeWitt AG, Pinto EM et al. MRI evaluation of lymphatic abnormalities in the neck and thorax after Fontan surgery: Relationship with outcome. Radiol 2019; 291: 774–780. DOI: 10.1148/radiol 2019.

14. Castellanos DA, Ahmad S, St. Clair N et al. Magnetic resonance three-dimensional steady-state free precession imaging of the thoracic duct in patients with Fontan circulation and its relationship to outcomes. J Cardiovasc Magn Reson 2023; 25: 28. DOI: 10.1186/S12968-023-00937-W.

15. Holm-Weber T, Kristensen RE, Mohanakumar S, Hjortdal VE. Gravity and lymphodynamics. Physiol Rep 2022; 10: e15289. DOI: 10.14814/PHY2.15289.

16. Mohanakumar S, Telinius N, Kelly B et al. Morphology and Function of the Lymphatic Vasculature in Patients with a Fontan Circulation. Circ Cardiovasc Imaging 2019; 12: e008074. DOI: 10.1161/CIRCIMAGING.118.008074.

17. Kelly B, Mohanakumar S, Telinius N, Alstrup M, Alstrup M, Hjortdal V. Function of Upper Extremity Human Lymphatics Assessed by near-Infrared Fluorescence Imaging. Lymphat Res Biol 2020; 18: 226–231. DOI: 10.1089/lrb.2019.0041.

18. Mathematics A. ImageJ. 2016:1-23. https://imagej.nih.gov/ij/.

19. Mohanakumar S, Kelly B, Turquetto ALR et al. Functional lymphatic reserve capacity is depressed in patients with a Fontan circulation. Physiol Rep 2021; 9: e14862. DOI: 10.14814/PHY2.14862.

20. Witte MH, Dumont AE, Clauss RH, Rader B, Levine N, Breed ES. Lymph circulation in congestive heart failure: effect of external thoracic duct drainage. Circulation 1969; 39: 723–733. DOI: 10.1161/01.CIR.39.6.723.

21. Cullen S, Shore D, Redington A. Characterization of right ventricular diastolic performance after complete repair of Tetralogy of Fallot: Restrictive physiology predicts slow postoperative recovery. Circulation 1995; 91: 1782–1789. DOI: 10.1161/01.CIR.91.6.1782/FORMAT/EPUB.

22. Rychik J, Atz AM, Celermajer DS et al. Evaluation and Management of the Child and Adult With Fontan Circulation: A Scientific Statement from the American Heart Association. Circulation 2019; 140: E234–E284. DOI: 10.1161/CIR.0000000000000696.

23. Brogan TV, Finn LS, Pyskaty DJ et al. Plastic bronchitis in children: a case series and review of the medical literature. Pediatr Pulmonol 2002; 34: 482–487. DOI: 10.1002/PPUL.10179.

24. Mallula KK, Kenny D, Hijazi ZM. Transjugular melody valve placement in a small child with protein losing enteropathy. Catheter Cardiovasc Interv 2015; 85: 267–270. DOI: 10.1002/CCD.25487.

25. Datar SA, Johnson EG, Oishi PE et al. Altered lymphatics in an ovine model of congenital heart disease with increased pulmonary blood flow. Am J Physiol Lung Cell Mol Physiol 2011; 302: 530–540. DOI: 10.1152/AJPLUNG.00324.2011.

26. Feltes TF, Hansen TN, Timothy Feltes CF, Professor of Pediatrics and A, of Pediatrics P, Assistant. Effects of an Aorticopulmonary Shunt on Lung Fluid Balance in the Young Lamb. Int Pediatr Res Found Inc 1989; 26: 94–97. DOI: 10.1203/00006450-198908000-00004.

27. Raj JU, Hazinski TA, Bland RD. Effect of hypoxia on lung lymph flow in newborn lambs with left atrial hypertension. Am J Physiol - Hear Circ Physiol 1988; 254: H487–H493. DOI: 10.1152/AJPHEART.1988.254.3.H487.

28. Hansen TN, Haberkern CM, Hazinski TA, Bland RD. Lung fluid balance in hypoxic lambs. Pediatr Res 1984; 18: 434–440. DOI: 10.1203/00006450-198405000-00009.

29. Boehme JT, Morris CJ, Chiacchia SR et al. HIF-1α promotes cellular growth in lymphatic endothelial cells exposed to chronically elevated pulmonary lymph flow. Sci Rep 2021; 11: 1–14. DOI: 10.1038/s41598-020-80882-1.

30. Morfoisse F, Renaud E, Hantelys F, Prats AC, Garmy-Susini B. Role of hypoxia and vascular endothelial growth factors in lymphangiogenesis. Mol Cell Oncol 2015; 2: 24821. DOI: 10.1080/23723556.2015.

31. Kristensen R, Kelly B, Kim E, Dori Y, Hjortdal VE. Lymphatic Abnormalities on Magnetic Resonance Imaging in Single-Ventricle Congenital Heart Defects Before Glenn Operation. J Am Hear Assoc Cardiovasc Cerebrovasc Dis 2023; 12: 29376–29376. DOI: 10.1161/JAHA.123.